Biomedicine & Pharmacotherapy 144 (2021) 112278

Contents lists available at ScienceDirect

Biomedicine & Pharmacotherapy

journal homepage: www.elsevier.com/locate/biopha

Longitudinal stability of molecular alterations and drug response profiles in tumor spheroid cell lines enables reproducible analyses

A.C. Nickel [a,1], D. Picard [b,c,d,l,1], N. Qin [b,c,d,l], M. Wolter [c], K. Kaulich [c], M. Hewera [a], D. Pauck [b,c], V. Marquardt [b,c], G. Torga [e], S. Muhammad [a], W. Zhang [f], O. Schnell [g], H.-J. Steiger [a], D. Hänggi [a], E. Fritsche [h], N.-G. Her [i], D.-H. Nam [j], M.S. Carro [g], M. Remke [b,c,d,l], G. Reifenberger [c,d,l], U.D. Kahlert [a,k,*]

[a] Department of Neurosurgery, University Hospital Düsseldorf and Medical Faculty, Heinrich Heine University Düsseldorf, Germany
[b] Department of Pediatric Oncology, Hematology and Clinical Immunology, University Hospital Düsseldorf and Medical Faculty, Heinrich Heine University Düsseldorf, Germany
[c] Institute of Neuropathology, University Hospital Düsseldorf and Medical Faculty, Heinrich Heine University Düsseldorf, Germany
[d] German Cancer Research Center (DKFZ), Heidelberg, Germany
[e] Drug Development Unit, Sarah Cannon Research Institute, London, UK
[f] Department of Neurosurgery, Beijing Tiantan Hospital, Capital Medical University, Beijing, People's Republic of China
[g] Department of Neurosurgery, Medical Center and Faculty of Medicine, University of Freiburg, Freiburg, Germany
[h] Leibniz Research Institute for Environmental Medicine, Düsseldorf, Germany
[i] R&D Center, AIMEDBIO Inc., Seoul, South Korea
[j] Department of Neurosurgery, Samsung Medical Center, Sungkyunkwan University, Seoul 06351, South Korea
[k] Molecular and Experimental Surgery, Department of General, Visceral, Vascular, and Transplant Surgery, University Hospital Magdeburg, Magdeburg, Germany
[l] German Cancer Consortium (DKTK), Partner Site Essen/Düsseldorf, Düsseldorf, Germany

ARTICLE INFO

Keywords:
Glioblastoma
In vitro drug screening
Longitudinal molecular profiling
Tumor spheroids

ABSTRACT

The utility of patient-derived tumor cell lines as experimental models for glioblastoma has been challenged by limited representation of the *in vivo* tumor biology and low clinical translatability. Here, we report on longitudinal epigenetic and transcriptional profiling of seven glioblastoma spheroid cell line models cultured over an extended period. Molecular profiles were associated with drug response data obtained for 231 clinically used drugs. We show that the glioblastoma spheroid models remained molecularly stable and displayed reproducible drug responses over prolonged culture times of 30 *in vitro* passages. Integration of gene expression and drug response data identified predictive gene signatures linked to sensitivity to specific drugs, indicating the potential of gene expression-based prediction of glioblastoma therapy response. Our data thus empowers glioblastoma spheroid disease modeling as a useful preclinical assay that may uncover novel therapeutic vulnerabilities and associated molecular alterations.

1. Introduction

In vitro culturing of cancer cells derived from human tumor specimens is a standard method in cancer research. Historically, *in vitro* drug testing of cultured cancer cells led to the discovery of pharmacological approaches that translated into clinical beneficial treatments for various cancers [1,2]. More recently, *in vitro* drug testing on large collections of genetically characterized cancer cell lines was conducted to identify tumor type-specific or tumor-agnostic chemotherapies [3,4]. Interestingly, inconsistencies in drug response data among different studies using the same interventions and the same cell models were identified, launching the debate whether classic cancer cell lines can still serve as a suitable research tool in drug development projects [2,5]. With the recent advances in high-throughput molecular profiling and computational technologies, and in the wake of establishing guidelines how to interpret *in vitro* drug screening data, technical and biological confounders impacting the reproducibly of cancer cell line-based *in vitro* drug testing are increasingly identified. Our study follows this line of

* Correspondence to: University Hospital Düsseldorf and Medical Faculty, Heinrich Heine University Düsseldorf, Moorenstraße 5, 40225 Dusseldorf, Germany.
E-mail address: ulf.kahlert@med.ovgu.de (U.D. Kahlert).
[1] These authors contributed equally to this paper.

https://doi.org/10.1016/j.biopha.2021.112278
Received 16 August 2021; Received in revised form 29 September 2021; Accepted 29 September 2021
Available online 7 October 2021

research focusing on glioblastoma, the most common malignant primary brain tumor with an eminent need to identify more effective, personalized treatment options [6,7]. We applied glioblastoma stem cell-like spheroid modeling technology that is assumed to better recapitulate tumor pathophysiology as opposed to conventional monolayer cultures [8–10]. Specifically, we performed a longitudinal study with determination of molecular profiles and drug response data to 231 clinical approved drugs comparing early and late *in vitro* passages of seven established glioblastoma cell lines that spontaneously grow as tumor spheroids *in vitro* (30 passages, ranging between 200 and 250 days in culture). Our approach involved multi-omics profiling, including large-scale DNA methylation analysis, next generation sequencing-based genomic profiling, and whole transcriptome RNA sequencing [11,12], combined with semi-automated *in vitro* drug screening. Thereby, we aimed to assess the stability of molecular profiles and drug response data over time, and to identify gene expression-based predictors of response to specific drugs.

2. Material and methods

2.1. Cell line culture conditions

Glioblastoma cell lines spontaneously growing as spheroid cultures were generously provided by Vescovi (HSR-GBM1, hereafter named GBM1, Milan, Italy) [13]; Riggins (JHH520, RRID:CVCL_VT33, Baltimore, USA) [14,15]; Herold-Mende (NCH644,RRID:CVCL_X914, Heidelberg, Germany) [16,17], and Carro (BTSC 349, BTSC 268, BTSC 23 and BTSC 233, Freiburg, Germany) [18,19]. Detailed characteristics of these glioblastoma cell lines have been reported before [13–19]. GBM1, JHH520 and NCH644 were cultivated in neurosphere medium containing serum-free Dulbecco's modified Eagle medium and 30% F12 medium (both Gibco, ThermoFisher, Germany) supplemented with 2% B27 (Gibco BRL), 20 ng/ml bovine fibroblast growth factor (FGF, Peprotech, Rocky Hill, NJ), 20 ng/ml human epidermal growth factor (EGF, Peprotech), 5 μg/ml heparin (Sigma-Aldrich, St Louis, MO) and 1% Penicillin-Streptomycin mixture (Pen/Strep, Gibco), Cell lines BTSC23, BTSC233, BTSC349 and BTSC268 were cultured in neurobasal medium-A containing 2% B27-supplement, 1% N2-supplement (Gibco BRL), 20 ng/ml FGF (Peprotech), 20 ng/ml hEGF (Peprotech), 5 μg/ml heparin (Sigma-Aldrich, St. Louis, MO) and 1% Pen/Strep (Gibco BRL).

All cell lines were cultivated under standard cell culture conditions at 37 °C temperature and 5% carbon dioxide. The medium was regularly exchanged three times per week and the cellular spheres were separated twice weekly by incubating them in TrypLE (Gibco BRL) for 3 min, followed by stopping the reaction with 3–5 ml medium and a subsequent pelleting by centrifugation for 5 min at 200×*g*. The medium-TrypLE solution was replaced by fresh medium and the cells were further cultured in new T75 suspension culture flasks. The cells were regularly tested for the absence of mycoplasma contamination using a PCR-based method and cell lines were verified as authentic by short tandem repeat analysis (STR) at the local Institute for Forensic Medicine, University Hospital Düsseldorf, Germany.

2.2. Sample collection

Cell pellets for all further analysis were collected simultaneous on the day performing the drug screen to obtain a multi-OMICS overview at the specific time point. Cells were pelleted at 200×*g* for 5 min and washed twice with PBS. The pellets were then stored at − 80 °C for further analysis. The same sample collection was repeated after 30 passages. A passage was counted after detaching and separating the spheres into single cells using TrypLE for 3 min.

2.3. RNA sequencing analysis

Total RNA was extracted from snap-frozen cell pellets using the NucleoSpin RNA extraction kit (Macherey-Nagel, Germany) with DNaseI treatment according to manufactures protocol. RNA was quantified using the Qubit RNA HS Assay (Thermo Fisher Scientific, Germany) and RNA quality was measured as RNA quality number (RQN) by capillary electrophoresis using the Fragment Analyzer and the total RNA Standard Sensitivity Assay (Agilent Technologies, Inc. Santa Clara, USA). Only RNA samples with a RQN value reaching the minimum of 7 were used for RNA sequencing. The library preparation was performed according to the manufacturer's protocol using the VAHTS™ Stranded mRNA-Seq Library Prep Kit for Illumina® V2 (Vazyme, China). Briefly, 300 ng total RNA were used for mRNA capturing, fragmentation, the synthesis of cDNA, adapter ligation and library amplification. Bead purified libraries were normalized and finally sequenced on the HiSeq 3000 (Illumina Inc., USA) with a read setup of 1 × 150 bp. The bcl2fastq tool was used to convert the bcl files to fastq files as well for adapter trimming and demultiplexing. Data analyses on fastq files were conducted with CLC Genomics Workbench (version 10.1.1, QIAGEN, The Netherlands). The reads of all probes were adapter trimmed and quality trimmed (using the default parameters: bases below Q13 were trimmed from the end of the reads, ambiguous nucleotides maximal 2). Fastq files were imported into Partek Flow (Partek Incorporated, St. Louis, MO, USA). Quality analysis and quality control were performed on all reads to assess read quality and to determine the amount of trimming required (both ends: 13 bases 5′ and 1 base 3′). Trimmed reads were aligned against the hg38 genome using the STAR v2.4.1d aligner [20]. Unaligned reads were further processed using Bowtie 2 v2.2.5 aligner [21]. Finally, aligned reads were combined before quantifying the expression against the ENSEMBL (release 84) database using the Partek Expectation-Maximization algorithm and quantile normalized. Partek Flow default settings were used in all analyses.

2.4. DNA methylation array

Genomic DNA was extracted from cell pellets using the innuPREP DNA mini kit (Analytic Jena, Germany) according to manufacturer's instruction. 50 ng/μl of the DNA was hand in to be processed for the Infinium MethylationEPIC Array (Ilumina Inc., USA) at MolecularNeuropathology.org, the Genomics and Proteomics Core Facility in Heidelberg for performing the Infinium MethylationEPIC Array (Illumina Inc., USA). The data was used for molecular subgrouping, and copy number profiling and beta methylation values as described before [22] and further analyzed for possible correlation between all OMICS data sets and changes between long-term cultured cell lines. Raw.idat files were uploaded to MolecularNeuropatholog.org. In addition to the determination of tumor type, data were processed for DNA copy number analyses. For beta-value processing,.idat files were processed using Partek® Genomics Suite® software using the minimal functional normalization using 2 principal components, and both NOOB background and dye correction.

2.5. Glioma-tailored gene mutation panel

A customized glioma gene panel detecting 20 glioma-associated genes was performed according to Zacher et al. [23] with minor changes. The glioma panel consisted of 660 primer pairs covering the coding sequences or mutational hot spot regions of the following genes: *ATRX, BRAF, CDKN2A, CDKN2B, CDKN2C, CIC, EGFR, FUBP1, H3–3A, IDH1, IDH2, NF1, NF2, NRAS, PIK3CA, PIK3R1, PTEN, RB1, TERT* promoter and *TP53*. DNA was extracted using the Maxwell RSC Blood DNA Kit (Promega, Germany) and quantified using the QuantiFluor® ONE dsDNA System (Promega, Germany) followed by TaqMan RNase P Detection Reagents Kit (Life Technologies, Germany) using a StepOne Plus™ real-time PCR machine (Life Technologies, Germany). Library preparation was generated using the Ion AmpliSeq™ Library 2.0 Kit (Life Technologies, Germany) and the customized AmpliSeq™ glioma gene panel. Sequencing was performed on Ion S5$^{(TM)}$ (Life Technologies,

Germany) and aligned to the human reference genome GRC37 (hg19) using the Torrent Suite 5.12.1.0 software. The sequence and copy number variants analysis was performed using the software Ion Reporter v5.12.0.0, IGV v.2.5.0 [24] and NextGene Version 2.4.2.2.

2.6. Drug library, quantification of cell growth and proliferation

A drug library composed of 231 established chemotherapeutic agents and novel anti-cancer compounds was dispensed in 384-well plates (Corning, USA) using the Tecan D300e Digital Dispenser (Tecan, USA). Each drug was dispensed at different concentrations eventually leading to final drug concentrations between 32.5 nM and 25 μM after the application of 30 μl cell suspension. Plates loaded with the drug library were stored until needed at − 80 °C. Prior to seeding the cells into the drug coated plates, a growth curve of each single cell line was analyzed for calculating the best cell number for performing the screen. For the assay spheroids were treated with TrypLE (Gibco, Germany) and filtered through a 45 μm filter for obtaining single cells. Prior to dispension of 30 μl of cell suspension onto the prepared 384 well plates (MultiDrop Combi, Thermofisher Scientific, USA), we determined cell viability and proliferative capability (Ki-67) using a GUAVA MUSE cytometer (Count and Viability Assay and Ki67 Proliferation kit, Luminex, USA) and incubation for 72 h. Readout was performed using the CellTiter-Glo luminescent cell viability assay (Promega, Germany) according to manufactures protocol. In brief, this luminescence-based assay is quantifying the ATP inside the medium that is produced by the living cells. The CellTiter-Glo® reagent was diluted 1:1 with PBS and 30 μl was added into each well of the plate and incubated for 10 min in the dark. The luminescence readout was determined with the Spark plate reader (Tecan, USA). The AUC and IC50 were calculated for each drug and cell line.

2.7. Quantification and statistical analysis

All statistical analyses were performed using the Partek® Genomics Suite® software. Comparisons of distributions were performed using the paired *t*-test. P-values < 0.05 were considered statistically significant. Hierarchical clustering and subgroup affiliation of DNA methylation profiling, RNA sequencing and drug screen outcome was performed using the Partek® Genomics Suite® software by selecting 5% or 10% of the most changed values between cells x + 0 *vs* x + 30. Similarity Network Fusion (SNF), a computational method for data integration, was performed combining mRNA expression and DNA methylation data according to Wang et al. [25]. The efficiency of the tested drug library was evaluated by calculating AUC using an R programmed script. Significance was considered if $p < 0.05$. Gene expression and drug response data compendium was analyzed and networks generated through the use of QIAGEN's Ingenuity Pathway Analysis tool (IPA, www.qiagen.com/ingenuity). Drug response and transcriptome data of cell models from x + 0 time point was used for the analysis.

2.8. Data and code availability

The acquired data supporting the current study will be deposited in the public repository European Genome-Phenome Archive (GSE181315).

3. Results

3.1. DNA mutation profiling and classification into molecular glioblastoma subtypes

Identity of the glioblastoma spheroid models BTSC23, BTSC233, BTSC268, BTSC349, JHH520, NCH644 and GBM1 was confirmed by short tandem repeat (STR) analyses (Supplementary Table 1) and DNA mutation profiles in these cell lines were characterized by next generation sequencing of glioma-associated genes (Supplementary Table 2). All cell lines carried *TERT* promoter mutations. Furthermore, frequent mutations were detected in the *NF1* and/or *TP53* genes. None of the glioblastoma spheroid models carried mutations in the *IDH1*, *IDH2*, *H3–3A* and *BRAF* genes. In addition, following consensus molecular subtyping of clinical samples according to *Capper* et al. [26] and *Verhaak* et al. [27], we performed array-based DNA methylome analyses and characterized gene expression profiles using whole transcriptome sequencing (Fig. 1A and B). All spheroid culture models were assigned to molecular glioblastoma subgroups using the DNA methylome or transcriptome data, respectively (Table 1). Precise assignment to the established DNA methylome classes, however, was challenging as the models either corresponded in variable percentages to the GBM RTK I or GBM RTK II methylation classes (BTSC cell lines) or could not be matched to any DNA-methylation class with a sufficiently high classifier score (GBM1, JHH520, NCH644).

3.2. Longitudinal molecular profiling over extended culture times

To investigate whether the glioblastoma spheroid culture models remain molecularly stable or evolved during long-term culturing by reshaping their epigenetic and transcriptional landscapes, we analyzed the transcriptomes and DNA methylomes of the seven models at two distinct time points in culture with intervals of 200–250 days corresponding to 30 *in vitro* passages of each model. The starting passage number of the different lines varied from passage 10 (BTSC 23, 233, 268, 349) to passages around 40 for the other used lines (JHH520, GBM1, NCH644). Unsupervised hierarchical cluster analyses of the transcriptome (Fig. 1A) and DNA methylome data sets (Fig. 1B) revealed minor differences with increasing time in culture in individual cell models, however, the profiles by-and-large remained stable, except for BTSC349 where several overall changes were detected in the methylome and transcriptome profiles. Overall, the mRNA expression of DNA methyltransferase 1 (*DNMT1*) changed significantly between the earlier and later passages of the seven models with almost 2-fold (1.86; $p = 0.0003$) increased expression in the later passages. Similarity Network Fusion (SNF) analysis using the transcriptome and DNA methylome data was then conducted to discern the biological heterogeneity or similarity of the individual models analyzed at different time points in culture. This analysis confirmed that the glioblastoma spheroid cell lines do not tend to undergo major changes during prolonged *in vitro* culturing time (Fig. 1C). We next were interested which genes are changed in the two models showing the least similarity between the two time points (BTSC233 and BTSC349). Notably, only the marginal number of $n = 15$ genes exhibited differential mRNA expression levels by more than 2-fold (paired *t*-test) between pooled early and late passages (Supplementary Table 3).

3.3. Determination and reproducibility of in vitro drug response patterns

To determine whether the molecularly stable glioblastoma spheroid models may also serve as reproducible models for functional studies, the response of each model to clinically approved drugs (chemical library specifications can be found in Supplementary Table 4) was investigated at the low passage (x + 0 passages) and at the high passage numbers (x + 30 passages). No phenotypic differences in between the two time points in terms of cell growth and viability as well as cellular proliferation were detected (viability: 80–97%; Ki67-positive 50–90%, Supplementary Figs. 1 and 2). In line, scatterplots for six of the seven models indicated a consistent response pattern to most inhibitors comparing early and late drug screening time points (R-value between 0.628 and 0.824, $p < 0.0001$ in all models, Fig. 2A). The cell line BTSC23 was excluded from the scatterplots as drug testing on passage x + 30 was not successful due to the slow growth of this model precluding expansion of the culture to the cell number needed for the performance of the screen. Since all other models showed an overall similarity in drug response

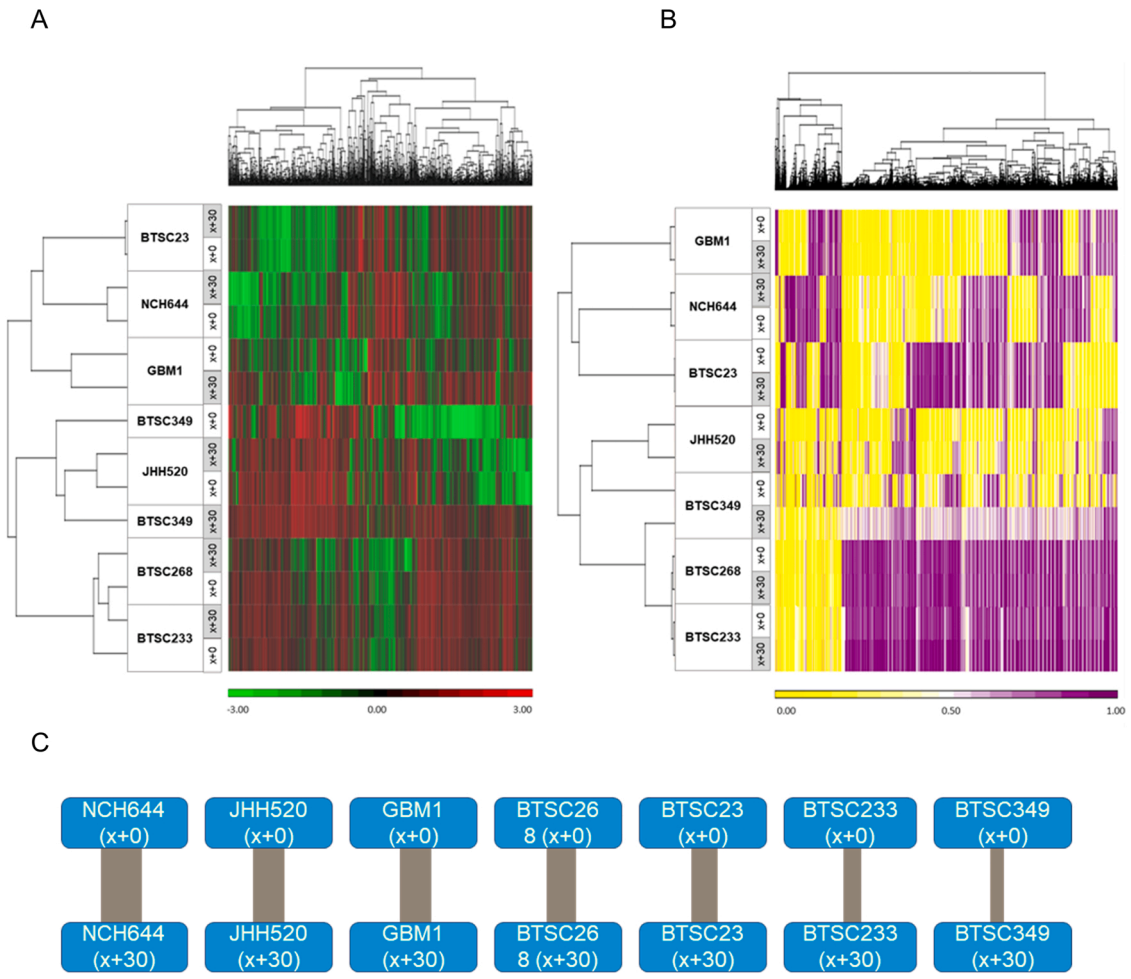

Fig. 1. Gene expression and DNA methylation profiles of the investigated glioblastoma spheroid models. (A) Results of unsupervised hierarchical clustering analysis based on gene expression profiles; green: downregulated genes, red: upregulated genes. (B) Results of hierarchical clustering analysis based on DNA-methylome profiles; yellow: unmethylated CpG sites, white to violet: methylated CpG sites. (C) Similarity Network Fusion (SNF) analysis was performed using the transcriptome and DNA methylome data to visualize similarities between passage x + 0 and x + 30. The stronger the connecting lines between the culture passages, the closer they are related. (For interpretation of the references to color in this figure legend, the reader is referred to the web version of this article.)

Table 1
Molecular classification of glioblastoma spheroid cell lines based on DNA methylation or mRNA expression profiles. Gene expression and DNA methylation profiles were used to classify each model into the respective transcriptional subgroups of glioblastoma, *i.e.* proneural (PN), classical (CL) or mesenchymal (MES), according to *Verhaak* et al. [27], as well as DNA-methylation-based subclasses, *i.e.*, receptor tyrosin kinase I (GBM RTKI) or RTK II/classical (GBM RTK II), according to *Capper* et al. [26]). If a sample could not be clearly assigned to a single DNA methylation subclass, the percentages matching to the individual subclasses are shown.

Cell model	DNA-methylation		Transcriptome	
	X + 0	X + 30	X + 0	X + 30
BTSC 23	RTK I (74%) RTK II (22%)	RTK I (78%) RTK II (18%)	PN	
BTSC 233	RTK I (27%) RTK II (61%)	RTK I (28%) RTK II (64%)	CL	
BTSC 268	RTK I (43%) RTK II (55%)	RTK I (29%) RTK II (59%)	CL	
BTSC 349	RTK I (34%) RTK II (34%)	RTK I (31%) RTK II (57%)	MES	
GBM1	no match		CL	
JHH520	no match		MES	
NCH644	no match		PN	

PN: pro-neural; CL: classical; MES: mesenchymal.

between earlier and later passages, we identified drugs that had the most pronounced effects on selected models but were less effective in other models. Scoring of substance effectivity was achieved by quantification of the area under the curve (AUC) in our cell growth-to-drug concentration graphs followed by averaging the calculated AUCs per intervention. The lower the AUC value, the more effective the drug was to the respective glioma cells. As a consequence, we determined approximately half of the drugs did cause a significant reduction in cell growth (Fig. 2B). Selecting the five drugs representing different prominent anticancer drug classes, namely bortezomib, ganetespib, dinaciclib, homoharringtonine, romidepsin, that represent inhibitors of cycline dependent kinases (CDK), heat shock protein 90/HSP90 and histone acetylates, we found that – although to different extent – almost all models were sensitive against bortezomib, ganetespib and dinaciclib treatment and approximately half of the models were inhibited in their growth when treated with either homoharringtonine or romidepsin (AUC values see Supplementary Table 5).

3.4. Association of in vitro drug response patterns with molecular profiles

Having identified groups of glioblastoma spheroid models that were responsive or non-responsive to selected drugs, we tried to identify potentially underlying molecular mechanism by using the Ingenuity Pathway Analysis tool (IPA; Qiagen). We deduced underlying therapy

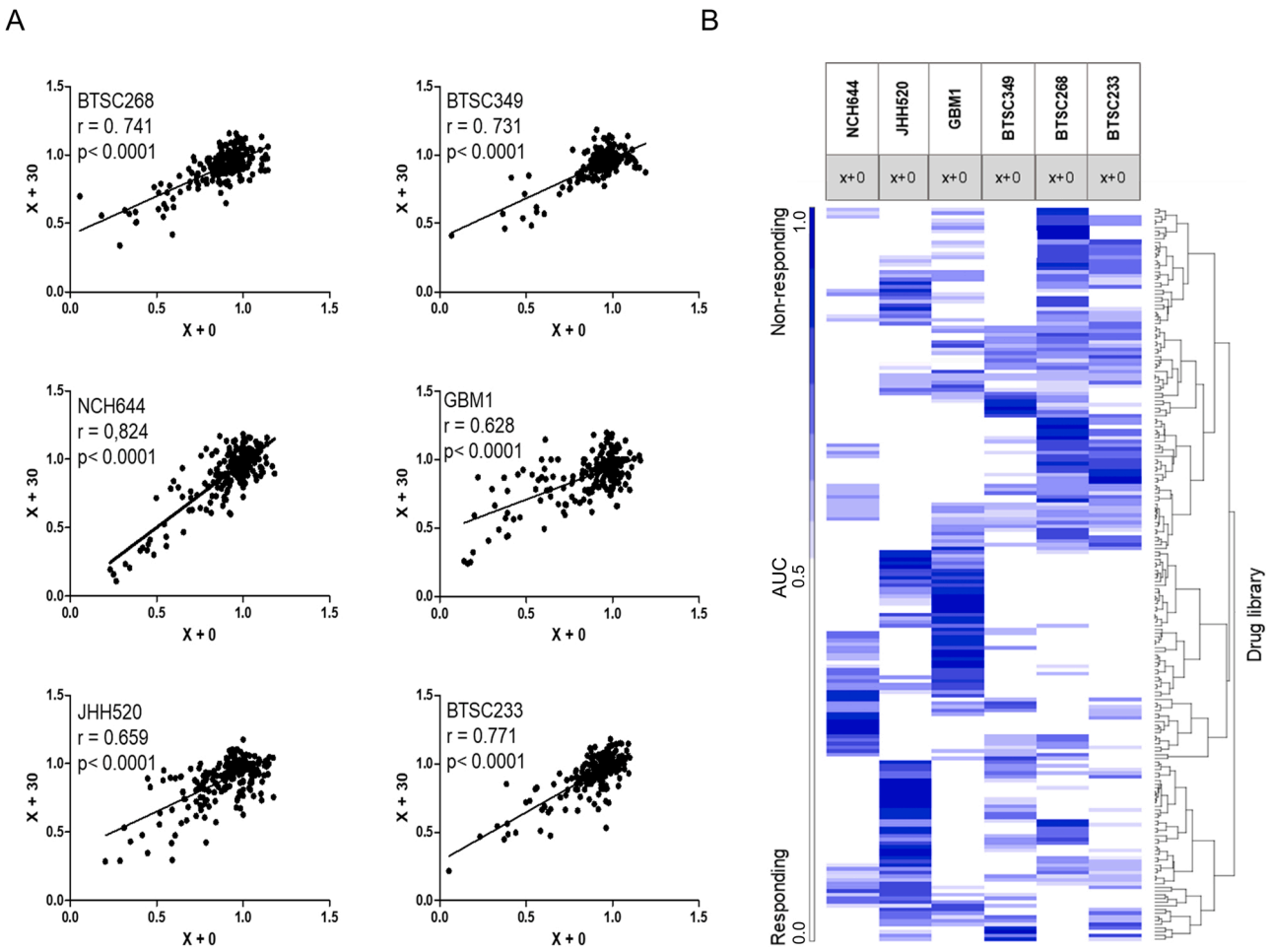

Fig. 2. Results of *in vitro* drug testing of the investigated glioblastoma spheroid models at different culture time points. (A) Scatterplots showing responses to each of the 231 compounds of the investigated drug library in the six cell lines with available data at the two passages x + 0 *vs.* x + 30. (B) Unsupervised hierarchical clustering of the cell lines at passages x + 0 based on their viability response to the 231 active compounds of the drug library revealing cell line unique overall response profiles. Differences in the drug responses were identified by quantifying the area under the curve (AUC) of cell growth drug concentration graphs. An AUC value below 0.5 indicates sensitivity of a cell to a given intervention with white to light blue colors indicating high to low sensitivity, and darker blue colors coding for less or lack of response to the respective drugs (AUC higher than 0.5, as indicted with scale bar on left). (For interpretation of the references to color in this figure legend, the reader is referred to the web version of this article.)

resistance mechanisms focusing on candidates from three different prominent classes of pharmaco-intervention. Focusing on the treatments with dinaciclib, ganetespid and romidepsin we used the spheroid model-specific transcriptome/drug response data compendium from the earlier test time point to conduct IPA. Applying the postulated therapy sensitivity-predicting gene signatures (exact listing of genes and their mean fold changed expression in sensitive cells compared to resistant cells can be found in Supplementary Table 6) enabled us to rank our cell models – at both test time points – from sensitive to high resistant cells (Fig. 3). Examples of drug resistance predicting transcriptional changes are: For dinaciclib, almost all models resistant to this drug were characterized by upregulated expression of *PIK3R1*, which could lead to suppressed signaling towards CDKs and thereby might cause resistance [28–30]. Resistant cell models showed a higher expression of *ELL2* transcripts. ELL2 is known to contribute to endoplasmic reticulum stress-mediated cell death and the unfolded protein response, which generally represents an adaptive pro-survival mechanism. Concerning sensitivity towards the HSP90 inhibitor ganetespid, we found that platelet-derived growth factor alpha (*PDGFRA*) transcript levels were lower in sensitive cells. Moreover, mRNA expression levels of pathway activating members of the Wingless (WNT) signaling pathway were found to be significantly downregulated in cells sensitive to the HDAC inhibitor romidepsin. Both PDGFRA and WNT signaling are prominent markers for stemness in glioma, generally accepted to be involved in mediating therapy resistance in this disease [31,32].

4. Discussion

The present study comprises a multi-OMICS molecular profiling approach combined with automated drug testing of patient-derived glioblastoma spheroid cell lines. These models more closely represent the 3D growth conditions in primary glioblastoma tissues and hence are considered advantageous to commonly used glioma cell lines cultured as monolayers [8–10]. To assess molecular and functional stability of the glioblastoma spheroid models, we performed the investigations at two distinct time points differing by 30 passages of *in vitro* culturing. In addition, we performed integrative analyses of the obtained molecular and functional datasets to identify potential associations of specific gene signatures with the response of glioblastoma cells to certain drugs. Glioblastoma spheroid lines may show *in vitro* culture-related differences in their DNA methylome in comparison to primary tumor specimens, which may further evolve upon extended *in vitro* propagation [33]. DNA methylation has been shown to alter during cell culture already in early passages which may explain why the profiles of these cells did not match with glioblastoma methylation profiles obtained from primary tissue specimens [33–35]. Consequently, we were not able

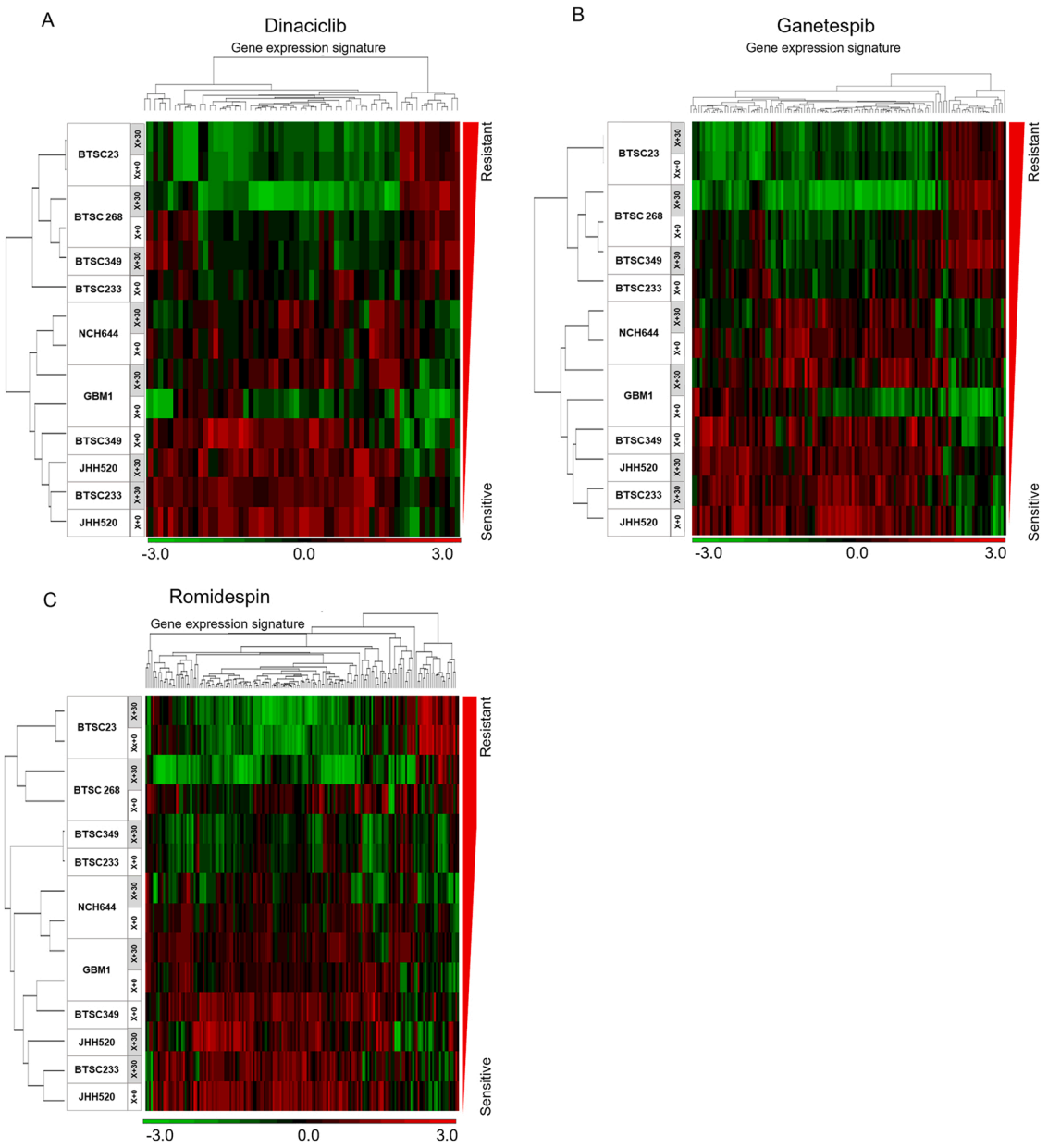

Fig. 3. Comparisons of *in vitro* drug response to selected drugs and gene expression data in the investigated glioblastoma spheroid models. Ingenuity pathway analysis (IPA, Qiagen) using transcriptome and drug response data identified differentially regulated genes associated to variations in drug resistances (gene lists and differential expression levels in resistant *vs.* sensitive models can be found in Supplementary Table 6). Focusing on substances (A) dinaciclib, (B) ganetespib and (C) romidepsin, representing three different prominent anti-cancer drug classes demonstrating differential activity, clustering the cells according to the identified gene expression signatures enables a ranking of our longitudinal assessed cell models also for their resistance to the respective drug intervention. Color coding: green: downregulated gene expression by up to − 3-fold, red: upregulated gene expression by up to 3-fold. (For interpretation of the references to color in this figure legend, the reader is referred to the web version of this article.)

to unequivocally assign the investigated spheroid models to the methylation-based subclasses of glioblastoma according to Capper et al. [27]. However, transcriptional classification according to *Verhaak* et al. [26] was maintained and showed marginal differences across the individual models. These results might be counterintuitive as classification according to the DNA methylation patterns is assumed to reflect the cell of origin and hence to be more stable when compared to transcriptome-based classification, which would be expected to be less stable and more rapidly adapting to different environmental conditions. Our results show that glioblastoma spheroid cell lines represent molecularly stable *in vitro* models allowing for reproducible functional analyses such as large-scale drug screening. Previously, larger anti-cancer drug screening studies raised concerns on the reproducibility of drug testing results using classic cancer cell lines [5,36,37]. Our experimental data provides evidence of molecular stability and reproducibility of drug testing results over *in vitro* passaging and clearly support the use of glioblastoma spheroid cell lines as faithful *in vitro* models. Indeed, our data indicate that the use of spheroid models may minimize reproducibility issues, although particular caution needs to be taken by using standardized procedures, regular quality controls [38], and essentially following the recommendations by the Global Biological Standards Institute concerning reproducibility concerns in biomedical research [39].

The comparison of molecular profiles with cellular drug response data allowed us to evaluate possible computational predictions of biological drug response. In particular, we provide evidence that response

of glioblastoma spheroid cell lines to the CDK inhibitor dinaciclib is linked to differential expression of a limited set of transcripts including *PIK3R1* and elongation factor for RNA polymerase II (*ELL2)*. The possible resistance or sensitivity mode of action for *PIK3R1* could be the direct influence on the X-box binding protein 1 (*XBP1) [*40 *{Park, 2010 #510]*. The respective gene product dictates the progression of UPR, and it is likely that the pathway cannot be blocked to the same extent in resistant cells as in the responsive models that showed higher mRNA expression of *XPB1* [41]. Similar mechanism could be true in the models that were sensitive to dinaciclib showing elevated *ELL2* levels. ELL2 has been reported to be involved in signaling following inhibition of CDKs by dinaciclib [28,42,43]. Resistance to HSP90 inhibitors were reported in cancers with altered activation of PDGFRA [44]. Interestingly, PDGFRA is a prominent client of HSP90, also in glioblastoma, and expression of PDGFRA was shown to mediate sensitivity of cancer cells for antibiotic-based HSP blockade [45]. Our data suggest that PDGFRA expression may influence stress resistance to ganetespib with reduced activity and increased cell vulnerability. Lastly, WNT signaling is known to regulate many molecular networks involved in therapy resistance in glioblastoma [46], and reducing the activity of this pathway in glioma cells emerges as a clinical relevant strategy to improve treatment of brain cancer patients [47]. HDAC inhibitors may represent an option to treat glioblastoma stem cell populations [48]. However, little is known on WNT mediating resistance to HDAC inhibitors. Our data suggest that reduced expression of WNT pathway members can contribute to increased sensitivity to the HDAC inhibitor romidepsin.

A possible limitation of our study relates to the use of established glioblastoma spheroid lines, which did not allow for comparative analyses of primary cultures or very early *in vitro* passages with later cultures after propagation over 30 or more *in vitro* passages. Some of the glioma cell lines used in this study have been reported to be aneuploid [16,49–51]. However, we did not determine the karyotype of each model investigated here. Hence, we cannot state whether the presented data on stability of molecular and drug response profiles in glioblastoma spheroid cell lines applies to both aneuploid and diploid models.

In conclusion, our data indicate that glioblastoma spheroid cell lines maintained under neural stem cell conditions remain molecularly stable over prolonged *in vitro* passaging and represent a robust model for reproducible identification of novel therapeutic vulnerabilities of this disease, as well as for the characterization of mechanisms of drug sensitivity and predictive molecular signatures.

CRediT authorship contribution statement

A.C. Nickel: Investigation, Visualization, Writing – original draft. **D. Picard:** Investigation, Formal analysis, Visualization. **N. Qin:** Resources. **M. Wolter:** Writing – review & editing, Resources. **K. Kaulich:** Resources. **M. Hewera:** Resources. **D. Pauck:** Writing – review & editing, Resources. **V. Marquardt:** Resources. **G. Torga:** Writing – review & editing. **S. Muhammad:** Writing – review & editing. **W. Zhang:** Writing – review & editing. **O. Schnell:** Writing – review & editing. **H.J. Steiger:** Writing – review & editing. **D. Hänggi:** Writing – review & editing. **E. Fritsche:** Funding acquisition. **M.S. Carro:** Resources. **M. Remke:** Resources. **G. Reifenberger:** Writing – review & editing. **U.D. Kahlert:** Conceptualization, Writing – original draft, Writing – review & editing, Supervision, Funding acquisition.

Conflict of interest statement

The authors declare that they have no known competing financial interests or personal relationships that could have appeared to influence the work reported in this paper.

Acknowledgments

This study was funded by the German Federal Ministry of Education and Research (BMBF KZ03VP03791/92). J. Wang, Hong Kong University of Science and Technology, is acknowledged for fruitful discussions. We also would like to thank Gabriele Brockerhoff and Ulrike Hübenthal for the preparation and printing of the drug test plates. Furthermore, we like to thank Kübra Taban and Mara Maue, both Heinrich-Heine Medical Faculty and University Hospital Düsseldorf, Germany for their support of the *in vitro* drug screening experiments.

Appendix A. Supporting information

Supplementary data associated with this article can be found in the online version at doi:10.1016/j.biopha.2021.112278.

References

[1] R.H. Shoemaker, The NCI60 human tumour cell line anticancer drug screen, Nat. Rev. Cancer 6 (10) (2006) 813–823, https://doi.org/10.1038/nrc1951.
[2] K.V. Kitaeva, C.S. Rutland, A.A. Rizvanov, V.V. Solovyeva, Cell culture based in vitro test systems for anticancer drug screening, Front. Bioeng. Biotechnol. 8 (2020) 322, https://doi.org/10.3389/fbioe.2020.00322.
[3] J. Barretina, G. Caponigro, N. Stransky, K. Venkatesan, A.A. Margolin, S. Kim, C. J. Wilson, J. Lehar, G.V. Kryukov, D. Sonkin, A. Reddy, M. Liu, L. Murray, M. F. Berger, J.E. Monahan, P. Morais, J. Meltzer, A. Korejwa, J. Jane-Valbuena, F. A. Mapa, J. Thibault, E. Bric-Furlong, P. Raman, A. Shipway, I.H. Engels, J. Cheng, G.K. Yu, J. Yu, P. Aspesi Jr., M. de Silva, K. Jagtap, M.D. Jones, L. Wang, C. Hatton, E. Palescandolo, S. Gupta, S. Mahan, C. Sougnez, R.C. Onofrio, T. Liefeld, L. MacConaill, W. Winckler, M. Reich, N. Li, J.P. Mesirov, S.B. Gabriel, G. Getz, K. Ardlie, V. Chan, V.E. Myer, B.L. Weber, J. Porter, M. Warmuth, P. Finan, J. L. Harris, M. Meyerson, T.R. Golub, M.P. Morrissey, W.R. Sellers, R. Schlegel, L. A. Garraway, The Cancer Cell Line Encyclopedia enables predictive modelling of anticancer drug sensitivity, Nature 483 (7391) (2012) 603–607, https://doi.org/10.1038/nature11003.
[4] M.J. Garnett, E.J. Edelman, S.J. Heidorn, C.D. Greenman, A. Dastur, K.W. Lau, P. Greninger, I.R. Thompson, X. Luo, J. Soares, Q. Liu, F. Iorio, D. Surdez, L. Chen, R.J. Milano, G.R. Bignell, A.T. Tam, H. Davies, J.A. Stevenson, S. Barthorpe, S. R. Lutz, F. Kogera, K. Lawrence, A. McLaren-Douglas, X. Mitropoulos, T. Mironenko, H. Thi, L. Richardson, W. Zhou, F. Jewitt, T. Zhang, P. O'Brien, J. L. Boisvert, S. Price, W. Hur, W. Yang, X. Deng, A. Butler, H.G. Choi, J.W. Chang, J. Baselga, I. Stamenkovic, J.A. Engelman, S.V. Sharma, O. Delattre, J. Saez-Rodriguez, N.S. Gray, J. Settleman, P.A. Futreal, D.A. Haber, M.R. Stratton, S. Ramaswamy, U. McDermott, C.H. Benes, Systematic identification of genomic markers of drug sensitivity in cancer cells, Nature 483 (7391) (2012) 570–575, https://doi.org/10.1038/nature11005.
[5] B. Haibe-Kains, N. El-Hachem, N.J. Birkbak, A.C. Jin, A.H. Beck, H.J. Aerts, J. Quackenbush, Inconsistency in large pharmacogenomic studies, Nature 504 (7480) (2013) 389–393, https://doi.org/10.1038/nature12831.
[6] R. Stupp, W.P. Mason, M.J. van den Bent, M. Weller, B. Fisher, M.J. Taphoorn, K. Belanger, A.A. Brandes, C. Marosi, U. Bogdahn, J. Curschmann, R.C. Janzer, S. K. Ludwin, T. Gorlia, A. Allgeier, D. Lacombe, J.G. Cairncross, E. Eisenhauer, R. O. Mirimanoff, European Organisation for Research and Treatment of Cancer Brain Tumor and Radiotherapy Groups, National Cancer Institute of Canada Clinical Trials Group, Radiotherapy plus concomitant and adjuvant temozolomide for glioblastoma, N. Engl. J. Med. 352 (10) (2005) 987–996, https://doi.org/10.1056/NEJMoa043330.
[7] C. Pauli, B.D. Hopkins, D. Prandi, R. Shaw, T. Fedrizzi, A. Sboner, V. Sailer, M. Augello, L. Puca, R. Rosati, T.J. McNary, Y. Churakova, C. Cheung, J. Triscott, D. Pisapia, R. Rao, J.M. Mosquera, B. Robinson, B.M. Faltas, B.E. Emerling, V. K. Gadi, B. Bernard, O. Elemento, H. Beltran, F. Demichelis, C.J. Kemp, C. Grandori, L.C. Cantley, M.A. Rubin, Personalized in vitro and in vivo cancer models to guide precision medicine, Cancer Discov. 7 (5) (2017) 462–477, https://doi.org/10.1158/2159-8290.CD-16-1154.
[8] J.D. Lathia, S.C. Mack, E.E. Mulkearns-Hubert, C.L. Valentim, J.N. Rich, Cancer stem cells in glioblastoma, Genes Dev. 29 (12) (2015) 1203–1217, https://doi.org/10.1101/gad.261982.115.
[9] N. Chaicharoenaudomrung, P. Kunhorm, W. Promjantuek, N. Rujanapun, N. Heebkaew, N. Soraksa, P. Noisa, Transcriptomic profiling of 3D glioblastoma tumoroids for the identification of mechanisms involved in anticancer drug resistance, In Vivo 34 (1) (2020) 199–211, https://doi.org/10.21873/invivo.11762.
[10] K.M. Wilson, L.A. Mathews-Griner, T. Williamson, R. Guha, L. Chen, P. Shinn, C. McKnight, S. Michael, C. Klumpp-Thomas, Z.A. Binder, M. Ferrer, G.L. Gallia, C. J. Thomas, G.J. Riggins, Mutation profiles in glioblastoma 3D oncospheres modulate drug efficacy, SLAS Technol. 24 (1) (2019) 28–40, https://doi.org/10.1177/2472630318803749.
[11] S. Chakraborty, M.I. Hosen, M. Ahmed, H.U. Shekhar, Onco-multi-OMICS approach: a new frontier in cancer research, Biomed. Res. Int. 2018 (2018), 9836256, https://doi.org/10.1155/2018/9836256.
[12] N. Zhao, Y. Liu, Y. Wei, Z. Yan, Q. Zhang, C. Wu, Z. Chang, Y. Xu, Optimization of cell lines as tumour models by integrating multi-omics data, Brief Bioinform. 18 (3) (2017) 515–529, https://doi.org/10.1093/bib/bbw082.
[13] A.L. Vescovi, E.A. Parati, A. Gritti, P. Poulin, M. Ferrario, E. Wanke, P. Frolichsthal-Schoeller, L. Cova, M. Arcellana-Panlilio, A. Colombo, R. Galli, Isolation and

cloning of multipotential stem cells from the embryonic human CNS and establishment of transplantable human neural stem cell lines by epigenetic stimulation, Exp. Neurol. 156 (1) (1999) 71–83, https://doi.org/10.1006/exnr.1998.6998.

[14] D.W. Parsons, S. Jones, X. Zhang, J.C. Lin, R.J. Leary, P. Angenendt, P. Mankoo, H. Carter, I.M. Siu, G.L. Gallia, A. Olivi, R. McLendon, B.A. Rasheed, S. Keir, T. Nikolskaya, Y. Nikolsky, D.A. Busam, H. Tekleab, L.A. Diaz Jr., J. Hartigan, D. R. Smith, R.L. Strausberg, S.K. Marie, S.M. Shinjo, H. Yan, G.J. Riggins, D. D. Bigner, R. Karchin, N. Papadopoulos, G. Parmigiani, B. Vogelstein, V. E. Velculescu, K.W. Kinzler, An integrated genomic analysis of human glioblastoma multiforme, Science 321 (5897) (2008) 1807–1812, https://doi.org/10.1126/science.1164382.

[15] Z.A. Binder, K.M. Wilson, V. Salmasi, B.A. Orr, C.G. Eberhart, I.M. Siu, M. Lim, J. D. Weingart, A. Quinones-Hinojosa, C. Bettegowda, A.B. Kassam, A. Olivi, H. Brem, G.J. Riggins, G.L. Gallia, Establishment and biological characterization of a panel of Glioblastoma Multiforme (GBM) and GBM variant oncosphere cell lines, PLoS One 11 (3) (2016), e0150271, https://doi.org/10.1371/journal.pone.0150271.

[16] B. Campos, F. Wan, M. Farhadi, A. Ernst, F. Zeppernick, K.E. Tagscherer, R. Ahmadi, J. Lohr, C. Dictus, G. Gdynia, S.E. Combs, V. Goidts, B.M. Helmke, V. Eckstein, W. Roth, P. Beckhove, P. Lichter, A. Unterberg, B. Radlwimmer, C. Herold-Mende, Differentiation therapy exerts antitumor effects on stem-like glioma cells, Clin. Cancer Res. 16 (10) (2010) 2715–2728, https://doi.org/10.1158/1078-0432.CCR-09-1800.

[17] N. Podergajs, N. Brekka, B. Radlwimmer, C. Herold-Mende, K.M. Talasila, K. Tiemann, U. Rajcevic, T.T. Lah, R. Bjerkvig, H. Miletic, Expansive growth of two glioblastoma stem-like cell lines is mediated by bFGF and not by EGF, Radio. Oncol. 47 (4) (2013) 330–337, https://doi.org/10.2478/raon-2013-0063.

[18] V. Fedele, F. Dai, A.P. Masilamani, D.H. Heiland, E. Kling, A.M. Gatjens-Sanchez, R. Ferrarese, L. Platania, D. Soroush, H. Kim, S. Nelander, A. Weyerbrock, M. Prinz, A. Califano, A. Iavarone, M. Bredel, M.S. Carro, Epigenetic regulation of ZBTB18 promotes glioblastoma progression, Mol. Cancer Res. 15 (8) (2017) 998–1011, https://doi.org/10.1158/1541-7786.MCR-16-0494.

[19] R. Ferrarese, G.Rt Harsh, A.K. Yadav, E. Bug, D. Maticzka, W. Reichardt, S. M. Dombrowski, T.E. Miller, A.P. Masilamani, F. Dai, H. Kim, M. Hadler, D. M. Scholtens, I.L. Yu, J. Beck, V. Srinivasasainagendra, F. Costa, N. Baxan, D. Pfeifer, D. von Elverfeldt, R. Backofen, A. Weyerbrock, C.W. Duarte, X. He, M. Prinz, J.P. Chandler, H. Vogel, A. Chakravarti, J.N. Rich, M.S. Carro, M. Bredel, Lineage-specific splicing of a brain-enriched alternative exon promotes glioblastoma progression, J. Clin. Investig. 124 (7) (2014) 2861–2876, https://doi.org/10.1172/JCI68836.

[20] A. Dobin, C.A. Davis, F. Schlesinger, J. Drenkow, C. Zaleski, S. Jha, P. Batut, M. Chaisson, T.R. Gingeras, STAR: ultrafast universal RNA-seq aligner, Bioinformatics 29 (1) (2013) 15–21, https://doi.org/10.1093/bioinformatics/bts635.

[21] B. Langmead, S.L. Salzberg, Fast gapped-read alignment with Bowtie 2, Nat. Methods 9 (4) (2012) 357–359, https://doi.org/10.1038/nmeth.1923.

[22] D. Capper, N.W. Engel, D. Stichel, M. Lechner, S. Gloss, S. Schmid, C. Koelsche, D. Schrimpf, J. Niesen, A.K. Wefers, D.T.W. Jones, M. Sill, O. Weigert, K.L. Ligon, A. Olar, A. Koch, M. Forster, S. Moran, O.M. Tirado, M. Sainz-Jaspeado, J. Mora, M. Esteller, J. Alonso, X.G. Del Muro, W. Paulus, J. Felsberg, G. Reifenberger, M. Glatzel, S. Frank, C.M. Monoranu, V.J. Lund, A. von Deimling, S. Pfister, R. Buslei, J. Ribbat-Idel, S. Perner, V. Gudziol, M. Meinhardt, U. Schuller, DNA methylation-based reclassification of olfactory neuroblastoma, Acta Neuropathol. 136 (2) (2018) 255–271, https://doi.org/10.1007/s00401-018-1854-7.

[23] A. Zacher, K. Kaulich, S. Stepanow, M. Wolter, K. Kohrer, J. Felsberg, B. Malzkorn, G. Reifenberger, Molecular diagnostics of gliomas using next generation sequencing of a glioma-tailored gene panel, Brain Pathol. 27 (2) (2017) 146–159, https://doi.org/10.1111/bpa.12367.

[24] J.T. Robinson, H. Thorvaldsdottir, W. Winckler, M. Guttman, E.S. Lander, G. Getz, J.P. Mesirov, Integrative genomics viewer, Nat. Biotechnol. 29 (1) (2011) 24–26, https://doi.org/10.1038/nbt.1754.

[25] B. Wang, A.M. Mezlini, F. Demir, M. Fiume, Z. Tu, M. Brudno, B. Haibe-Kains, A. Goldenberg, Similarity network fusion for aggregating data types on a genomic scale, Nat. Methods 11 (3) (2014) 333–337, https://doi.org/10.1038/nmeth.2810.

[26] D. Capper, D.T.W. Jones, M. Sill, V. Hovestadt, D. Schrimpf, D. Sturm, C. Koelsche, F. Sahm, L. Chavez, D.E. Reuss, A. Kratz, A.K. Wefers, K. Huang, K.W. Pajtler, L. Schweizer, D. Stichel, A. Olar, N.W. Engel, K. Lindenberg, P.N. Harter, A. K. Braczynski, K.H. Plate, H. Dohmen, B.K. Garvalov, R. Coras, A. Holsken, E. Hewer, M. Bewerunge-Hudler, M. Schick, R. Fischer, R. Beschorner, J. Schittenhelm, O. Staszewski, K. Wani, P. Varlet, M. Pages, P. Temming, D. Lohmann, F. Selt, H. Witt, T. Milde, O. Witt, E. Aronica, F. Giangaspero, E. Rushing, W. Scheurlen, C. Geisenberger, F.J. Rodriguez, A. Becker, M. Preusser, C. Haberler, R. Bjerkvig, J. Cryan, M. Farrell, M. Deckert, J. Hench, S. Frank, J. Serrano, K. Kannan, A. Tsirigos, W. Bruck, S. Hofer, S. Brehmer, M. Seiz-Rosenhagen, D. Hanggi, V. Hans, S. Rozsnoki, J.R. Hansford, P. Kohlhof, B. W. Kristensen, M. Lechner, B. Lopes, C. Mawrin, R. Ketter, A. Kulozik, Z. Khatib, F. Heppner, A. Koch, A. Jouvet, C. Keohane, H. Muhleisen, W. Mueller, U. Pohl, M. Prinz, A. Benner, M. Zapatka, N.G. Gottardo, P.H. Driever, C.M. Kramm, H. L. Muller, S. Rutkowski, K. von Hoff, M.C. Fruhwald, A. Gnekow, G. Fleischhack, S. Tippelt, G. Calaminus, C.M. Monoranu, A. Perry, C. Jones, T.S. Jacques, B. Radlwimmer, M. Gessi, T. Pietsch, J. Schramm, G. Schackert, M. Westphal, G. Reifenberger, P. Wesseling, M. Weller, V.P. Collins, I. Blumcke, M. Bendszus, J. Debus, A. Huang, N. Jabado, P.A. Northcott, W. Paulus, A. Gajjar, G. W. Robinson, M.D. Taylor, Z. Jaunmuktane, M. Ryzhova, M. Platten, A. Unterberg, W. Wick, M.A. Karajannis, M. Mittelbronn, T. Acker, C. Hartmann, K. Aldape, U. Schuller, R. Buslei, P. Lichter, M. Kool, C. Herold-Mende, D.W. Ellison, M. Hasselblatt, M. Snuderl, S. Brandner, A. Korshunov, A. von Deimling, S. M. Pfister, DNA methylation-based classification of central nervous system tumours, Nature 555 (7697) (2018) 469–474, https://doi.org/10.1038/nature26000.

[27] R.G. Verhaak, K.A. Hoadley, E. Purdom, V. Wang, Y. Qi, M.D. Wilkerson, C. R. Miller, L. Ding, T. Golub, J.P. Mesirov, G. Alexe, M. Lawrence, M. O'Kelly, P. Tamayo, B.A. Weir, S. Gabriel, W. Winckler, S. Gupta, L. Jakkula, H.S. Feiler, J. G. Hodgson, C.D. James, J.N. Sarkaria, C. Brennan, A. Kahn, P.T. Spellman, R. K. Wilson, T.P. Speed, J.W. Gray, M. Meyerson, G. Getz, C.M. Perou, D.N. Hayes, The Cancer Genome Atlas Research Network, Integrated genomic analysis identifies clinically relevant subtypes of glioblastoma characterized by abnormalities in PDGFRA, IDH1, EGFR, and NF1, Cancer Cell 17 (1) (2010) 98–110, https://doi.org/10.1016/j.ccr.2009.12.020.

[28] M.D. Galbraith, H. Bender, J.M. Espinosa, Therapeutic targeting of transcriptional cyclin-dependent kinases, Transcription 10 (2) (2019) 118–136, https://doi.org/10.1080/21541264.2018.1539615.

[29] T.T. Huang, E.J. Lampert, C. Coots, J.M. Lee, Targeting the PI3K pathway and DNA damage response as a therapeutic strategy in ovarian cancer, Cancer Treat. Rev. 86 (2020), 102021, https://doi.org/10.1016/j.ctrv.2020.102021.

[30] S.W. Park, Y. Zhou, J. Lee, A. Lu, C. Sun, J. Chung, K. Ueki, U. Ozcan, The regulatory subunits of PI3K, p85alpha and p85beta, interact with XBP-1 and increase its nuclear translocation, Nat. Med. 16 (4) (2010) 429–437, https://doi.org/10.1038/nm.2099.

[31] C. Cenciarelli, H.E. Marei, A. Felsani, P. Casalbore, G. Sica, M.A. Puglisi, A. J. Cameron, A. Olivi, A. Mangiola, PDGFRalpha depletion attenuates glioblastoma stem cells features by modulation of STAT3, RB1 and multiple oncogenic signals, Oncotarget 7 (33) (2016) 53047–53063, https://doi.org/10.18632/oncotarget.10132.

[32] Y. Lee, J.K. Lee, S.H. Ahn, J. Lee, D.H. Nam, WNT signaling in glioblastoma and therapeutic opportunities, Lab. Investig. 96 (2) (2016) 137–150, https://doi.org/10.1038/labinvest.2015.140.

[33] Y. Shen, C.J. Grisdale, S.A. Islam, P. Bose, J. Lever, E.Y. Zhao, N. Grinshtein, Y. Ma, A.J. Mungall, R.A. Moore, X. Lun, D.L. Senger, S.M. Robbins, A.Y. Wang, J. L. MacIsaac, M.S. Kobor, H.A. Luchman, S. Weiss, J.A. Chan, M.D. Blough, D. R. Kaplan, J.G. Cairncross, M.A. Marra, S.J.M. Jones, Comprehensive genomic profiling of glioblastoma tumors, BTICs, and xenografts reveals stability and adaptation to growth environments, Proc. Natl. Acad. Sci. USA 116 (38) (2019) 19098–19108, https://doi.org/10.1073/pnas.1813495116.

[34] S. Bork, S. Pfister, H. Witt, P. Horn, B. Korn, A.D. Ho, W. Wagner, DNA methylation pattern changes upon long-term culture and aging of human mesenchymal stromal cells, Aging Cell 9 (1) (2010) 54–63, https://doi.org/10.1111/j.1474-9726.2009.00535.x.

[35] H.A. Rogers, R. Chapman, H. Kings, J. Allard, J. Barron-Hastings, K.W. Pajtler, M. Sill, S. Pfister, R.G. Grundy, Limitations of current in vitro models for testing the clinical potential of epigenetic inhibitors for treatment of pediatric ependymoma, Oncotarget 9 (92) (2018) 36530–36541, https://doi.org/10.18632/oncotarget.26370.

[36] U. Ben-David, B. Siranosian, G. Ha, H. Tang, Y. Oren, K. Hinohara, C.A. Strathdee, J. Dempster, N.J. Lyons, R. Burns, A. Nag, G. Kugener, B. Cimini, P. Tsvetkov, Y. E. Maruvka, R. O'Rourke, A. Garrity, A.A. Tubelli, P. Bandopadhayay, A. Tsherniak, F. Vazquez, B. Wong, C. Birger, M. Ghandi, A.R. Thorner, J.A. Bittker, M. Meyerson, G. Getz, R. Beroukhim, T.R. Golub, Genetic and transcriptional evolution alters cancer cell line drug response, Nature 560 (7718) (2018) 325–330, https://doi.org/10.1038/s41586-018-0409-3.

[37] M. Niepel, M. Hafner, C.E. Mills, K. Subramanian, E.H. Williams, M. Chung, B. Gaudio, A.M. Barrette, A.D. Stern, B. Hu, J.E. Korkola, L. Consortium, J.W. Gray, M.R. Birtwistle, L.M. Heiser, P.K. Sorger, A multi-center study on the reproducibility of drug-response assays in mammalian cell lines, Cell Syst. 9 (1) (2019) 35–48, https://doi.org/10.1016/j.cels.2019.06.005.

[38] M. Hewera, A. Nickel, N. Knipprath, S. Muhammad, X. Fan, H. Steiger, D. Hänggi, U. Kahlert, Measures to increase value of preclinical research - an inexpensive and easy-to-implement approach to a QMS for an academic research lab [version 1; peer review: awaiting peer review], F1000Research 9 (660) (2020), https://doi.org/10.12688/f1000research.24494.1.

[39] L.P. Freedman, G. Venugopalan, R. Wisman, Reproducibility2020: progress and priorities, F1000Res 6 (2017) 604, https://doi.org/10.12688/f1000research.11334.1.

[40] J.N. Winnay, J. Boucher, M.A. Mori, K. Ueki, C.R. Kahn, A regulatory subunit of phosphoinositide 3-kinase increases the nuclear accumulation of X-box-binding protein-1 to modulate the unfolded protein response, Nat. Med. 16 (4) (2010) 438–445, https://doi.org/10.1038/nm.2121.

[41] T.K. Nguyen, S. Grant, Dinaciclib (SCH727965) inhibits the unfolded protein response through a CDK1- and 5-dependent mechanism, Mol. Cancer Ther. 13 (3) (2014) 662–674, https://doi.org/10.1158/1535-7163.MCT-13-0714.

[42] B. Garcia-Reyes, A.L. Kretz, J.P. Ruff, S. von Karstedt, A. Hillenbrand, U. Knippschild, D. Henne-Bruns, J. Lemke, The emerging role of Cyclin-Dependent Kinases (CDKs) in pancreatic ductal adenocarcinoma, Int. J. Mol. Sci. 19 (10) (2018), https://doi.org/10.3390/ijms19103219.

[43] M.P. Garcia-Cuellar, E. Fuller, E. Mathner, C. Breitinger, K. Hetzner, L. Zeitlmann, A. Borkhardt, R.K. Slany, Efficacy of cyclin-dependent-kinase 9 inhibitors in a murine model of mixed-lineage leukemia, Leukemia 28 (7) (2014) 1427–1435, https://doi.org/10.1038/leu.2014.40.

[44] B. Dewaele, B. Wasag, J. Cools, R. Sciot, H. Prenen, P. Vandenberghe, A. Wozniak, P. Schoffski, P. Marynen, M. Debiec-Rychter, Activity of dasatinib, a dual SRC/ABL kinase inhibitor, and IPI-504, a heat shock protein 90 inhibitor, against gastrointestinal stromal tumor-associated PDGFRAD842V mutation, Clin. Cancer

Res. 14 (18) (2008) 5749–5758, https://doi.org/10.1158/1078-0432.CCR-08-0533.
[45] D. Matei, M. Satpathy, L. Cao, Y.C. Lai, H. Nakshatri, D.B. Donner, The platelet-derived growth factor receptor alpha is destabilized by geldanamycins in cancer cells, J. Biol. Chem. 282 (1) (2007) 445–453, https://doi.org/10.1074/jbc.M607012200.
[46] U.D. Kahlert, J.V. Joseph, F.A.E. Kruyt, EMT- and MET-related processes in nonepithelial tumors: importance for disease progression, prognosis, and therapeutic opportunities, Mol. Oncol. 11 (7) (2017) 860–877, https://doi.org/10.1002/1878-0261.12085.
[47] A.K. Suwala, A. Hanaford, U.D. Kahlert, J. Maciaczyk, Clipping the wings of glioblastoma: modulation of WNT as a novel therapeutic strategy, J. Neuropathol. Exp. Neurol. 75 (5) (2016) 388–396, https://doi.org/10.1093/jnen/nlw013.
[48] R. Chen, M. Zhang, Y. Zhou, W. Guo, M. Yi, Z. Zhang, Y. Ding, Y. Wang, The application of histone deacetylases inhibitors in glioblastoma, J. Exp. Clin. Cancer Res 39 (1) (2020) 138, https://doi.org/10.1186/s13046-020-01643-6.
[49] A. Dirkse, A. Golebiewska, T. Buder, P.V. Nazarov, A. Muller, S. Poovathingal, N.H. C. Brons, S. Leite, N. Sauvageot, D. Sarkisjan, M. Seyfrid, S. Fritah, D. Stieber, A. Michelucci, F. Hertel, C. Herold-Mende, F. Azuaje, A. Skupin, R. Bjerkvig, A. Deutsch, A. Voss-Bohme, S.P. Niclou, Stem cell-associated heterogeneity in Glioblastoma results from intrinsic tumor plasticity shaped by the microenvironment, Nat. Commun. 10 (1) (2019) 1787, https://doi.org/10.1038/s41467-019-09853-z.
[50] S. Seton-Rogers, Glioblastoma: transforming fusions induce aneuploidy, Nat. Rev. Cancer 12 (9) (2012) 585, https://doi.org/10.1038/nrc3350.
[51] B. Boisselier, F. Dugay, M.A. Belaud-Rotureau, A. Coutolleau, E. Garcion, P. Menei, P. Guardiola, A. Rousseau, Whole genome duplication is an early event leading to aneuploidy in IDH-wild type glioblastoma, Oncotarget 9 (89) (2018) 36017–36028, https://doi.org/10.18632/oncotarget.26330.